ISBN: 978-3-95450-208-0 doi:10.18429/JACoW-IPAC2019-WEZPLS1

CONTROL OF LASER PLASMA ACCELERATED ELECTRONS: A ROUTE FOR COMPACT FREE ELECTRON LASERS

M. E. Couprie *, T. André, F. Blache, F. Briquez, F. Bouvet, Y. Dietrich, J. P. Duval, M. El-Ajjouri, A. Ghaith, C. Herbeaux, N. Hubert, C. Kitégi, M. Labat, N. Leclercq, A. Lestrade, A. Loulergue, O. Marcouillé, F. Marteau, D. Oumbarek, P. Rommeluère, M. Sebdaoui, K. Tavakoli, M. Valléau, Synchrotron SOLEIL, GIF-sur-YVETTE , France.
S. Corde, J. Gautier, J. P. Goddet, O. Kononenko, G. Lambert, A. Tafzi, K. Ta Phuoc, C. Thaury, Laboratoire d'Optique Appliquée, Palaiseau, France.
S. Bielawski, C. Evain, E. Roussel, C. Szwaj, Laboratoire PhLAM, Lille, France
I. Andriyash, V. Malka, Weizmann Institute, Israel
C. Benabderrahmane, ESRF, Grenoble, France

Abstract

The recent spectacular development of Laser Plasma Accelerators (LPA) that now can deliver GeV electron beams in an extremely short distance makes them very promising. Applications for light sources based on undulator radiation and Free Electron Laser (FEL) appear as an intermediate step to move from an acceleration concept to an accelerator qualification. However, the presently achieved divergence and energy spread require some electron beam manipulations. The COXINEL test line was designed for enabling FEL operation with baseline reference parameters. It comprises variable permanent magnet quadrupoles for divergence handling, a magnetic chicane for electron energy sorting, a second set of quadrupole for chromatic focusing and an undulator for synchrotron radiation emission and/or FELgain medium. The transport along the line is controlled [1]. The synchrotron radiation emitted by the undulator radiation is studied under different conditions of detection, electron beam manipulation and undulator parameters. These observations pave the way towards LPA based FEL.

INTRODUCTION

Accelerator based light sources presently know a very wide development [2]. After the first generation light sources (in the eighties) parasitically using synchrotron radiation from storage rings built for high energy physics, the construction of few mm.rad emittance dedicated storage rings accomodating few undulators [3] and wigglers (second generation), third generation light sources (from the nineties) with storage rings of low emittance, high undulator number, enabling partial transverse coherence are present workhorses for investigation of matter, biological and cultural heritage samples. Accelerator based light sources make a large use of undulators, providing a permanent periodic magnetic field B_u and period λ_u. In an undulator, relativistic electrons of Lorentz factor γ oscillate, and emit synchrotron radiation. The single electron radiation from the consecutive undulator periods constructively interferes, leading to a spectrum of sharp lines at the resonance wavelength λ_r and its harmonics of order n, given by $\lambda_r = \lambda_u(1 + K_u^2/2 + \gamma^2\theta^2)/2n\gamma^2$, with K_u the deflection parameter (K_u = 93.4 B_u[T] λ_u[m]), θ the observation angle, with a Full Width Half Maximum (FWHM) homogeneous relative linewidth of $(\frac{\Delta\lambda}{\lambda})_{\text{hom}} \simeq \frac{0.9}{nN_u}$ with N_u the undulator number of periods. The emission from the $2N_u$ sources and the interference process leads to an increase of brightness with respect to dipole radiation. The quality of the electron beam (low energy spread and emittance) is essential to preserve the interference effect even in the case of multi-electron contribution. The path towards increased spectral brightness follows two approaches. Besides the reduction of the emittance on "diffraction limited storage rings" [4] for improved transverse coherence, longitudinal coherence can be achieved by setting the electrons in phase (micro-bunching while wiggling in an undulator), thanks to the Free Electron Laser process [5]. FELs use more generally linear accelerators for short wavelength operation, enabling to provide very short pulse and small spectral bandwidth. The advent of X-ray FELs [6] led to an increase of the peak brightness by several orders of magnitude, enabling to decipher the matter evolution on ultra fast time scales.

Presently, beam manipulation strategies are developed to shape the FEL pulse for advanced properties, approaching further the diffraction and Fourier limits in a wide spectral range with a high level of flexibility for users. Alternately, the use of advanced acceleration concepts such as LPA [7], are considered to qualify them with the FEL applications, with the goal of achieving «more compact» light sources [8, 22]. An LPA based FEL would combine two major outcomes of the laser invention [9]. Following Chirped Pulse Amplification techniques [10], ultra high power lasers can now create and accelerate electrons up to several GeV within ultra-short distances [11–13]. An intense laser focused onto a gas target ionizes the gas medium and pushes the electrons out of its path while leaving the ions undisturbed in comparison to electrons within the timescale larger than plasma wave formation. An induced intense electric field of the plasma drags behind the laser pulse. The electron beam seeded in the acceleration phase of the plasma wave is accelerated until it surpasses the wave and reaches it maximum energy. The development LPA is promising: GeV range energy, kA

* couprie@synchrotron-soleil.fr

ISBN: 978-3-95450-208-0 doi:10.18429/JACoW-IPAC2019-WEZPLS1

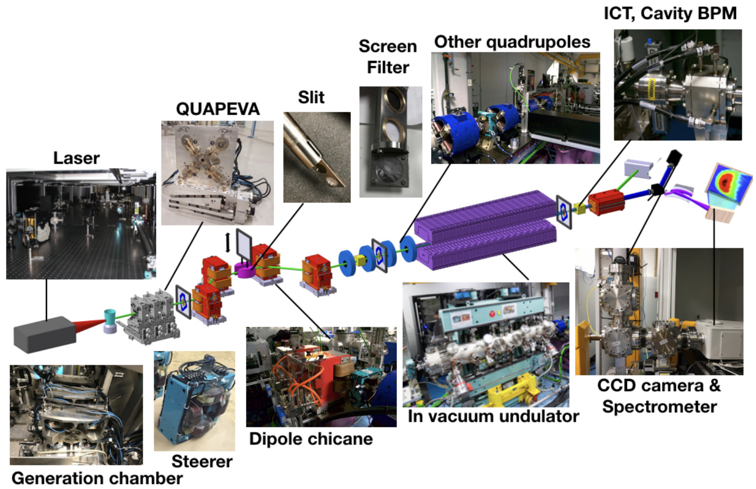

Figure 1: Sketch of the COXINEL line : Laser hutch (grey), gas jet (blue), QUAPEVA high gradient permanent magnet quadrupoles (grey), electromagnetic dipole based chicane (red) with a plunger for inserting an electron imager or a slit, quadruplet of electromagnetic quadrupoles (blue), undulator (purple) surrounded by two steerers and removable screens for electron imaging, electron dipole dump (red), electron imager, photon diagnostics (CCD camera and spectrometer). Associated built equipment.

peak current, ultra-short bunches, 1π mm.mrad normalized emittance beams can be produced. These features are generally not achieved all together. The hopes put in LPA to drive undulator radiation and FEL light sources are challenged by LPA parameters that do not meet conventional accelerator state-of-the-art performance. While conventional accelerators deliver μrad divergence and per mille of energy spread beams, the LPA large energy spread and divergence require to mitigate chromatic effects [14, 15], that can lead to a dramatic emittance growth and afferent beam quality degradation in the transfer lines. The LPA based undulator radiation observed so far [16–19] does not present the quality in terms of spectral purity and stability as currently achieved on conventional accelerators, mainly because of the electron beam characteristics. Demonstration of a proper electron beam control is the first challenge to overcome in the path towards LPA based FELs. Large divergence requires strong focusing right after the electron source, with high gradient permanent magnet quadrupoles [20]. Large energy spread can be handled by a decompression chicane [21, 22] or a transverse gradient undulator [23, 24]. Advantage can even be taken by the correlation energy position introduced by the chicane [25]. In the frame of the LUNEX5 project of advanced compact free electron laser demonstrator [26, 27] in France, the ERC Advanced Grant COXINEL program [28] aims at demonstrating FEL amplification with the help of a dedicated transport line to handle and manipulate the beam properties.

COXINEL LINE

The COXINEL line has been designed and built at Synchrotron SOLEIL [29], for being installed at Laboratoire d'Optique Appliquée (LOA), where a Ti:Sapphire laser system delivering 1.5 J, 30 fs FWHM pulses can be used for the experiment. The LPA development is carried out at LOA in the frame of an ERC Advanced Grant X-FIVE. The layout of the COXINEL line on the page is illustrated in Fig. 1. The COXINEL manipulation line has been designed considering baseline reference parameters for 200 and 400 MeV, as given in Table 1 for the 180 MeV case.

Table 1: COXINEL Baseline Reference Case at the Source and at the Undulator After Beam Manipulation

Slice Parameters	Source	Undulator
Divergence	1 mrad	0.1 mrad
Beam size	1 μm	50 μm
Bunch length (rms)	3.3 fs	33 fs
Charge	34 pC	34 pC
Peak Current	4.4 kA	440 A
Slice energy spread σ_γ	1% rms	0.1% rms
Normalised emittance ϵ_N	1 mm.mrad	1.7 mm.mrad

The divergence is rapidly mitigated (5 cm away from the source) via strong focusing with a triplet of variable permanent magnet based quadrupoles (so-called QUAPEVA), as shown in Fig. 2. The QUAPEVAs present a variable strength (via rotating cylindrical magnet surrounding a central Halbach ring quadrupole [30]) and an adjustable magnetic center position (via translation tables) [31,32]. A magnetic chicane then longitudinally stretches the beam, sorts electrons in energy and selects the energy range of interest via a removable and adjustable slit mounted in the middle of the chicane.

ISBN: 978-3-95450-208-0 doi:10.18429/JACoW-IPAC2019-WEZPLS1

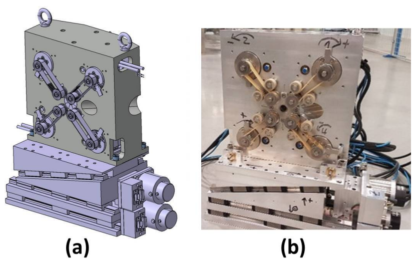

Figure 2: QUAPEVA variable permanent magnet quadrupoles : (a) mechanical design, (b) built device.

A second set of quadrupoles matches the beam inside an in-vacuum undulator (typical SOLEIL 2 m long U20 (period 20 mm), cryo-ready U18 (period 18 mm) or 3 m long cryo-ready U15 (period 15 mm)) [33–36]. The electron beam can be monitored with current transformers and cavity beam position monitors or by inserting scintillator screens (Lanex and Yag) along the line [37]. The ”200 MeV” corresponds to undulator radiation in the UV, while the 400 MeV case associated to the U15 cryogenic undulator enables to reach the VUV spectral range. The different components of the line have been built or purchased and characterized [38, 39], as illustrated in Fig. 1. A picture of the line installed in the ”Salle Jaune” at LOA is shown in Fig. 3. An iris for the LPA laser, the transfer line components, the undulator, and an iris at the line exit are aligned within $\pm$ 100 μm on the same axis with a laser tracker. A reference green laser is used for daily alignement. A seed for the FEL using the High order Harmonic Generation process [40] can be prepared from another branch of the infra-red laser.

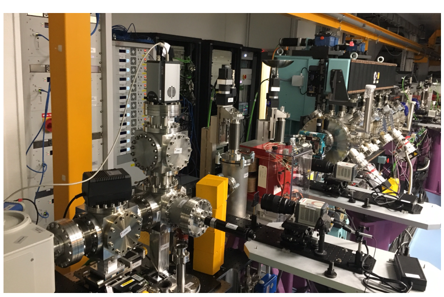

Figure 3: Picture of the installed COXINEL line (end part) : U18 undulator, dipole dump (red), photon diagnostics.

The electron optics, a source to image optics, refocuses the beam inside the undulator thanks to the strong gradient QUAPEVA [25]. The electron transport, modeled using the BETA code, has been benchmarked with ASTRA [41] including collective effects, ELEGANT and OCELOT. The total emittance growth is frozen at the exit of the QUAPEVA triplet. The emittance is then dominated by the chromatic emittance, scaling as the square of the initial divergence and proportional to the energy spread, and remains then unaffected along the line. The seeded FEL is computed using GENESIS, and is achievable considering baseline reference parameters [25], as illustrated in Fig. 4. Different variant of electron beam beam optics are considered. The so-called ”supermatching optics” enables to focus each electron beam slice in synchronisation with the progression of the amplified synchrotron radiation along the undulator, taking advantage of the energy / position correlation introduced in the chicane. Specific optics focusing on the different screens implemented along the line are designed for the beam transport experiments for more precise measurements. Finally, an optics enabling to focus also the beam vertically in the chicane equipped with a slit permits to clean the large energy spread beam. The sensitivity study of the FEL versus different parameters has been carried out [42].

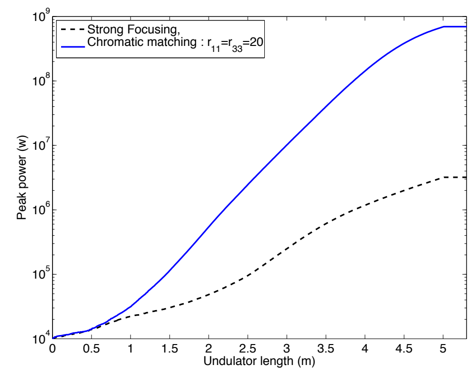

Figure 4: FEL amplification in the case of the COXINEL 400 MeV baseline parameters for a 5 m long U15 undulator, for the strong focusing and supermatching optics, figure from Ref. [25].

THE PRODUCED ELECTRON BEAM CHARACTERIZATION

The 1.5 J, 30 FWHM fs pulse laser is focused into a supersonic jet of $He-N_2$ gas mixture for the LPA to operate in the robust ionisation injection [43]. The beam is first characterized with an electron spectrometer, using a permanent magnet dipole and a Lanex screen. An example is displayed in Fig. 5 (left). Produced beams range up to 250 MeV in a broad energy spectrum. The charge density deduced from the calibration of the electron spectrometer is typically 0.5 pC / MeV. This wide spectrum and associated charge density significantly deviate from the base line reference parameters (see Table 2). The electron spectrometer enables also to measure the vertical divergence, and few mrad divergence (1.2-5 mrad RMS (Root Mean Square)) are achieved, depending on the COXINEL run and day. The electron beam image can be measured with a screen inserted 0.56 m away from the source, and the vertical divergence is generally larger than the one from the spectrometer which does not capture low energy electrons. The ratio of the vertical to horizontal size is used to rescale the vertical divergence distribution versus energy from the spectrometer data to provide the horizontal divergence one. Electron beam pointing fluctuations and drift as large as 1.5 mrad RMS can be observed. They might result from the laser itself or from intrinsic features of

ISBN: 978-3-95450-208-0 doi:10.18429/JACoW-IPAC2019-WEZPLS1

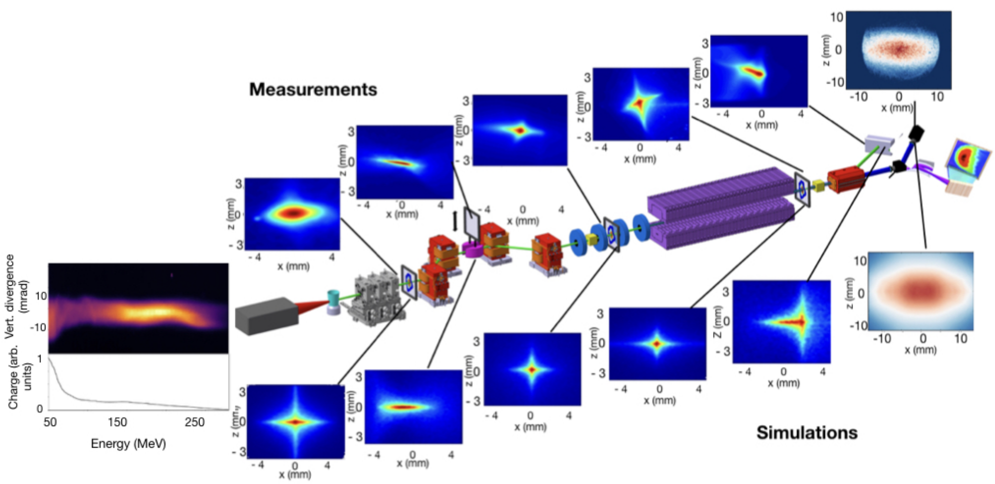

Figure 5: COXINEL electron and photon beam measurements compared to simulations. Left : electron beam spectrometer measurements and transverse distributions along the screens implemented on the line (up : measurements, down : simulations using the measured electron beam distribution as an input). Right : undulator radiation transverse pattern (measured with on a CCD camera and modeled using the transported electron beam without electron energy selection with a slit in the chicane). Case of an initial vertical divergence of 3.5 mrad-RMS with a standard deviation of 0.3 mrad over 20 shots, slice divergence in the 176 ± 5 MeV energy range of 3.5 mrad-RMS with a standard deviation of 0.2 mrad over 20 shots.

the LPA source. They are much larger than the ± 100 μm pre-alignment of the COXINEL line.

Table 2: Baseline Electron Reference Parameters Compared to the Measured Ones, 180 MeV Case at the Source Point

Parameters	Baseline	Measured
Vertical divergence (mrad)	1	1.2-5
Horizontal divergence (mrad)	1	1.8-7.5
Charge density (pC/MeV)	5	0.5
RMS energy spread σ_γ (%)	1	>15

THE ELECTRON BEAM TRANSPORT

After a first rough beam transport along the line where chromatic effects play an important role, a Beam Position Alignment Compensation strategy based on the matrix response approach is developed to mitigate alignement residual errors and pointing drifts [1]. The beam dispersion and position can be independently corrected thanks to a proper setting of the QUAPEVA magnetic axis via the translation tables on which they are mounted. The alignment is then performed step by step, along the different electron imaging screens, with the adjustment of the electron beam position and vertical dispersion at the chicane center, followed by the positions and horizontal dispersion at the undulator entrance and exit. The QUAPEVA strength is then slightly adjusted to optimize the focusing thanks to the rotation of the cylindrical magnets. The matched transported beam measurements agree with simulations for measured beam characteristics (dipole spectrometer and observation on a screen), as displayed in Fig. 5. The focused beam, both measured and simulated, also exhibits a cross-like shape which is a signature of the chromatic effects (different electron beam energies being focused at different longitudinal positions).

THE MEASURED UNDULATOR RADIATION

The transported electron beam is then suitable for the observation of the undulator synchrotron radiation. The 107 period U18 hybrid cryo-ready undulator is used for first observations of synchrotron radiation. Built and measured at Synchrotron SOLEIL, it consists of $Pr_2Fe_{14}B$ (CR53-Hitachi) magnets Vanadium of 1.32 T remanence field and 1.63 T coercivity and of Vanadium Permendur poles. For an energy of 176 MeV, the resonant wavelength is 200 nm at 5 mm gap and spans between 180 and 280 nm while varying the gap.

First undulator radiation measurements are carried out using a CCD camera installed 3 m away from the exit of the undulator. The broad energy spectrum electron beam is transported along the line without selection in the chicane. The low energy electrons are filtered along the line, resulting in an energy spread of 30 % RMS. Because of the broad range of electron energies, the resonant wavelength spans over 100-360 nm for a 5 mm gap, with 200 nm for the reference energy of 176 MeV. Figure 5 (right) displays the measured and modeled radiation flux density normalized to 1 pC focused on the CDD, collecting on and off-axis radiation. They present a similar shape and signal level. The integrated intensity shown in Fig. 6 over the photon transverse beam shape for wavelengths above 150 nm (due to the optics system transmission) is then measured versus undulator gap g. For larger gaps, the resonant wavelength decreases (since ($K_u \propto \exp(-\pi g/\lambda_u)$)). The camera receives on-axis radiation from the range of resonant wavelengths, and their harmonics, with their associated red shifted off-axis radia-

ISBN: 978-3-95450-208-0 doi:10.18429/JACoW-IPAC2019-WEZPLS1

tion ($(\theta\gamma)^2$ term in the undulator wavelength expression). The signal follows qualitatively the decrease of the undulator total power versus gap, as $exp(-2\pi g/\lambda_u)$ in the detection spectral range.

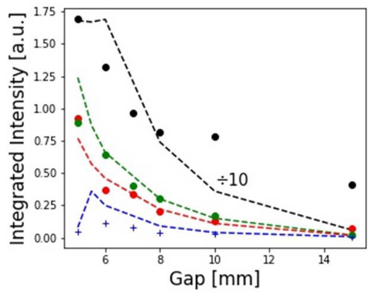

Figure 6: Integrated intensity measured by the CCD camera (points) and computed using SRW (dashed). Black : without optical filter, red: with a 300 nm bandpass filter (45 nm bandwidth), green : with a 254 nm optical filter (38 nm bandwidth), blue: with a 200 nm filter (10 nm bandwidth).

Because of the wide energy range of the electron beam distribution resulting from the ionization injection scheme, a slit is introduced in the chicane, with a limited charge reduction of the electrons at the energy of interest, while suppressing the low and high energy content of the distribution. For a 4 mm width slit in the chicane, the RMS energy spread drops to 8 % RMS, without significant charge reduction for the energy of interest. Such an optics enables to limit the inhomogeneous contribution of the energy spread to the spectral purity of the radiation. A rough spectral analysis can be carried out inserting various bandpass filters in front of the CCD camera. As shown in Fig. 6, the intensity drops when the optical filters are applied. The radiation collected through the 253 and 300 nm filters is mainly off-axis, and its intensity decreases versus gap in a similar manner as for the total power. In the case of the 200 nm filter centered on the resonant wavelength at the reference energy for the 5 mm gap, the intensity is maximized at 6 mm including some off-axis radiation, as expected from undulator radiation theory [44]. SRW [45] simulations present a similar behavior with the measurements. The full estimated number of photons per beam charge N_{ph} is $\approx 3.10^7$ pC^{-1}.

A more precise spectral analysis can be carried out using a spectrometer equipped with a CCD camera. A typical spectrum is displayed in Fig. 7. The radiation linewidth can be controlled using the electron beam energy selection via the slit in the chicane.

CONCLUSION

We have shown that the LPA electron beam properties can be manipulated through an adequate transport line, mitigating the performance that do not meet the one of state-of-the-art conventional accelerators for some-specific applications. These results can be applied for various LPA applications, such as undulator synchrotron radiation, free electron laser and the new generation of colliders, requiring stages of LPA

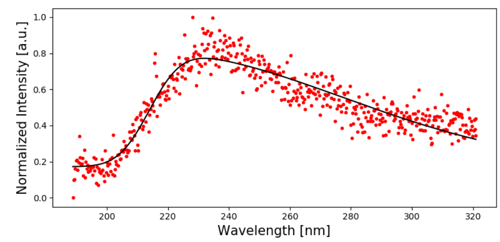

Figure 7: Undulator spectral flux measured with the Horiba iHR 320 spectrometer at 5 mm gap (3 mm electron slit).

accelerating modules or free electron laser applications. The transported electron beam on COXINEL has enabled successful measurement of undulator radiation under various conditions. The possibility to observe FEL amplification strongly depends on the LPA beam parameters that can be experimentally achieved, and the qualification of the LPA with an FEL application still remains a major present Graal.

ACKNOWLEDGEMENTS

The authors are very grateful for the support of the European Research Council (ERC) for COXINEL (340015, P. I. M. E. Couprie), X-Five (339128, PI: V.Malka), the EuPRAXIA design study (653782) and the Fondation de la Cooperation Scientifique (QUAPEVA-2012-058T). They also thank the support of SOLEIL and LOA staff.

REFERENCES

[1] T. André, T. *et al.* "Control of laser plasma accelerated electrons for light sources", Nat. Comm., vol. 9, pp. 1334, 2018.

[2] M. E. Couprie, J. M. Filhol, "X radiation sources based on accelerators", *Comptes Rendus Phys.*, vol. 9:487–506, 2008.

[3] A. Hofmann, "Quasi-monochromatic synchrotron radiation from undulators", *Nucl. Instrum. Meth.*, vol. 152, p. 17–21, 1978.

[4] M. Eriksson, J. F. van der Veen, C. Quitmann, "Diffraction-limited storage rings–a window to the science of tomorrow", *Journal of synchrotron radiation*, vol. 21, p. 837–842, 2014.

[5] J. M. Madey, "Stimulated emission of bremsstrahlung in a periodic magnetic field", *Jour. Appl. Phys.*, vol. 42, p. 1906–1913, 1971.

[6] P. Emma et al., "First lasing and operation of an Ångstrom-wavelength free-electron laser", *Nature Photonics*, vol. 4, p. 641, 2010.

[7] T. Tajima and J. M. Dawson, "Laser electron accelerator", *Phys. Rev. Lett.*, vol. 43, p. 267–270, Jul 1979.

[8] F. Gruner et al., " Design considerations for table-top, laser-based VUV and X-ray free electron lasers", *Appl. Phys. B*, vol. 86, p. 431–435, 2007.

[9] A. L. Schawlow and C. H. Townes, "Infrared and optical masers", *Physical Review*, vol. 112, no. 6, p. 1940, 1958.

[10] D. Strickland and G. Mourou, "Compression of amplified chirped optical pulses", *Optics communications*, vol. 55, no. 6, p. 447-449, 1985.

ISBN: 978-3-95450-208-0 doi:10.18429/JACoW-IPAC2019-WEZPLS1

[11] E. Esarey, C. Schroeder, and W. Leemans, "Physics of laser-driven plasma-based electron accelerators" , *Reviews of Modern Physics*, vol. 81, no. 3, p. 1229, 2009.

[12] V. Malka *et al.*, "Laser-driven accelerators by colliding pulses injection: A review of simulation and experimental results", *Physics of Plasmas*, vol. 16, no. 5, p. 056703, 2009.

[13] W P. Leemans *et al.*, "Multi-GeV electron beams from capillary-discharge-guided subPetaWatt laser pulses in the self-trapping regime", *Phys. Rev. Lett.*, vol. 113, p. 245002, 2014.

[14] K. Floettmann, "Some basic features of the beam emittance", *Phys. Rev. ST Accel. Beams*, vol. 6, p. 034202, 2003.

[15] M. Migliorati *et al.*, "Intrinsic normalized emittance growth in laser-driven electron accelerators", *Phys. Rev. ST Accel. Beams*, vol. 16, p. 011302, 2013.

[16] H. P. Schlenvoigt *et al.*, "A compact synchrotron radiation source driven by a laser-plasma wakefield accelerator", *Nature Physics*, vol. 4, no. 2, pp. 130–133, 2008.

[17] M. Fuchs *et al.*, "Laser-driven soft-X-ray undulator source," *Nature physics*, vol. 5, no. 11, pp. 826–829, 2009.

[18] G. Lambert *et al.*, "Progress on the generation of undulator radiation in the UV from a plasma-based electron beam", *Proceed. FEL conf., Nara, Japan*, p. 2, 2012.

[19] M.P. Anania *et al.*, "An ultrashort pulse ultra-violet radiation undulator source driven by a laser plasma wakefield accelerator", *Appl. Phys. Lett.*, vol. 104, no. 26, pp. 264102, 2014.

[20] A. Ghaith, D. Oumbarek, M. Valléau, F. Marteau, M. E. Couprie, "Permanent Magnet-Based Quadrupoles for Plasma Acceleration Sources", *Instruments*, vol. 3, no. 2, pp. 27, 2019.

[21] A. Maier, A. Meseck, S. Reiche, C. Schroeder, T. Seggebrock, and F. Gruener, "Demonstration scheme for a laser-plasma-driven free-electron laser", *Physical Review X*, vol. 2, no. 3, p. 031019, 2012.

[22] M. E. Couprie, A. Loulergue, M. Labat, R. Lehe, and V. Malka, "Towards a free electron laser based on laser plasma accelerators", *Journal of Physics B: Atomic, Molecular and Optical Physics*, vol. 47, no. 23, p. 234001, 2014.

[23] T. I. Smith, J. M. J. Madey, L.R. Elias, and D.A.G. Deacon, "Reducing the sensitivity of a free-electron laser to electron energy", *Journal of Applied Physics*, vol. 50, no. 7, pp. 4580–4583, 1979.

[24] Z. Huang, Y. Ding, C. B. Schroeder "Compact X-ray free-electron laser from a laser-plasma accelerator using a transverse-gradient undulator", *Phys. Rev. Lett.*, vol. 109, no. 20, pp. 204801, 2012.

[25] A. Loulergue, M. Labat, C. Evain, C. Benabderrahmane, V. Malka, and M. Couprie, "Beam manipulation for compact laser wakefield accelerator based free-electron lasers", *New Journal of Physics*, vol. 17, no. 2, p. 023028, 2015.

[26] M.-E. Couprie *et al.*, "The LUNEX5 project in France", *Jour. of Physics: Conf. Series*, vol. 425, no. 7, pp. 072001, 2013.

[27] M. Couprie *et al.*, "Strategies towards a compact XUV free electron laser adopted for the LUNEX5 project", *Journal of Modern Optics*, vol. 63, no. 4, pp. 1–13, 2015.

[28] M. Couprie *et al.*, "Experiment preparation towards a demonstration of laser plasma based free electron laser amplification", *Proc. FEL'14 (Basel, Switzerland)*, 2014.

[29] M. E. Couprie *et al.*, "An application of laser–plasma acceleration: towards a free-electron laser amplification," *Plasma Phys. Cont. Fusion*, vol. 58, no. 3, p. 034020, 2016.

[30] K. Halbach *et al.*, "Design of permanent multipole magnets with oriented rare earth cobalt material," *Nucl. Instrum. Meth.*, vol. 169, p. 1–10, 1980.

[31] F. Marteau *et al.*, "Variable high gradient permanent magnet quadrupole (QUAPEVA)", *Applied Physics Letters*, vol. 111, p. 253503, 2017.

[32] A. Ghaith *et al.*, "Tunable high gradient quadrupoles for a laser plasma acceleration based FEL", *Nucl. Instrum. Meth. A*, vol. 909, p. 290-293, 2018.

[33] C. Benabderrahmane *et al.* "Development of a 2 m $Pr_2Fe_{14}B$ cryogenic permanent magnet undulator at SOLEIL", *Jour. of Physics: Conf. Series*, vol. 425, no. 3, p. 032019, 2013.

[34] M. E. Couprie *et al.* "Cryogenic undulators", *Advances in X-ray Free-Electron Lasers Instrumentation III*, vol. 9512, no. 3, p. 951204, 2015.

[35] M. Valléau *et al.*, "Development of cryogenic undulators with PrFeB magnets at SOLEIL", *AIP Conference Proceedings*, vol. 1741, no. 1, p. 020024, 2016.

[36] C. Benabderrahmane *et al.* "Development and operation of a $Pr_2Fe_{14}B$ based cryogenic permanent magnet undulator for a high spatial resolution x-ray beam line", *Phys. Rev. Acc. Beams*, vol. 20, no. 3, p. 033201, 2017.

[37] M. Labat, M. El Ajjouri, N. Hubert, T. André, A. Loulergue, M. E. Couprie "Electron and photon diagnostics for plasma acceleration-based FELs", *Journal of synchrotron radiation*, vol. 25, no. 1, p. 59–67, 2018.

[38] M. E. Couprie *et al.*, " An application of laser–plasma acceleration: towards a free-electron laser amplification", "*Plasma Phys. Cont. Fusion*, vol. 58, no. 3, pp. 034020, 2016.

[39] M. E. Couprie *et al.*, "Towards free electron laser amplification to qualify laser plasma acceleration", *The review of laser engineering*, vol. 45, no. 2, pp. 94–98, 2017.

[40] A. L'Huillier, P. Balcou, "High-order harmonic generation in rare gases with a 1-ps 1053-nm laser", *Phys. Rev. Lett.*, vol. 70, no. 6, p. 774, 1993.

[41] M. Khojoyan *et al.*, " Transport studies of LPA electron beam towards the FEL amplification at COXINEL", *Nucl. Instrum. Meth. A*, vol. 829, no. 2, pp. 260-264, 2016.

[42] M. Labat *et al.*, "Robustness of a plasma acceleration based Free Electron Laser", *Phys. Rev. Acc. Beams*, vol. 21, no. 11, pp. 114802, 2018.

[43] C. McGuffey *et al.*, "Ionization induced trapping in a laser wakefield accelerator", *Phys. Rev. Lett.*, vol. 104, no. 2, p. 025004, 2010.

[44] P. Elleaume, H. Onuki, "Wigglers and their Applications", *Taylor and Francis, London*, 2003.

[45] O. Chubar and P. Elleaume, "Accurate and Efficient Computation of Synchrotron Radiation in the Near Field Region", in *Proc. 6th European Particle Accelerator Conf. (EPAC'98)*, Stockholm, Sweden, Jun. 1998, paper THP01G, pp. 1177–1179.